J Therm Anal Calorim (2010) 100:867–871
DOI 10.1007/s10973-010-0720-1

Synthesis, characterization, infrared studies, and thermal analysis of $Mn_{0.6}Zn_{0.4}Fe_2(C_4H_2O_4)_3{\cdot}6N_2H_4$ and its decomposition product $Mn_{0.6}Zn_{0.4}Fe_2O_4$

U. B. Gawas · S. C. Mojumdar · V. M. S. Verenkar

CTAS2009 Special Chapter

Abstract Manganese zinc ferrous fumarato–hydrazinate precursor, $Mn_{0.6}Zn_{0.4}Fe_2(C_4H_2O_4)_3{\cdot}6N_2H_4$ was synthesized for the first time and characterized by chemical analysis, infrared spectral studies, and thermal analysis. Infrared studies show band at 977 cm^{-1} indicating bidentate bridging nature of the hydrazine in the complex. Thermogravimetric (TG) studies show two steps dehydrazination followed by two steps total decarboxylation. The precursor on touching with burning splinter undergoes self propagating autocatalytic decomposition yielding ultrafine $Mn_{0.6}Zn_{0.4}Fe_2O_4$. XRD studies confirms single phase formation as well as nanosize nature of "as prepared" $Mn_{0.6}Zn_{0.4}Fe_2O_4$. The saturation magnetization of the "as prepared" $Mn_{0.6}Zn_{0.4}Fe_2O_4$ was found to be 31.46 emu gm^{-1}, which is lower than the reported, confirms the ultrafine nature of the oxide.

Keywords Hydrazine precursor · Ultrafine oxide · Autocatalytic decomposition · DSC · TG · XRD

Introduction

Mixed metal carboxylates and dicarboxylates have attracted the attention of number of researchers since these complexes serves as precursor for many technologically important materials [1–13]. Hydrazine by virtue of its positive heat of formation is thermodynamically unstable. Practically, however, it is quite stable and can be handled safely [14]. Hydrazine can support a flame by its decomposition alone and can act as a monopropellant [15]. Coordination of hydrazine to the metal carboxylates markedly lowers the decomposition temperature of the metal carboxylates and yields nanosize metal oxides at comparatively lower temperatures. For this reason, hydrazinated complex of metal as well as mixed metal carboxylates and dicarboxylates have been used for the synthesis of technologically important materials like γ-Fe_2O_3 [16–18], ferrites [19, 20], manganites [21–24], cobaltites [25], etc.

Among hydrazinates of metal carboxylates and dicarboxylates which have been used for the synthesis of metal as well as mixed metal oxides are formates [26], acetates [27, 28], oxalates [29, 30], malonates and succinates [31–35], maleates [33, 35], tartrates [35], malates [35, 36], and fumarates [37–44]. In the present study, we are reporting, synthesis, and characterization of manganese zinc ferrous fumarato–hydrazinate precursor and its decomposition product, $Mn_{0.6}Zn_{0.4}Fe_2O_4$.

Experimental

Preparation of manganese zinc ferrous fumarato–hydrazinate

The method given below for the preparation of manganese zinc ferrous fumarato–hydrazinate precursor has been dealt with in detail, elsewhere [37, 38]. In this method, a requisite quantity of sodium fumarate in aqueous medium was stirred with hydrazine hydrate (99–100%) in an inert atmosphere for 2 h. To this solution, a stoichiometric

U. B. Gawas · V. M. S. Verenkar
Department of Chemistry, Goa University, Taleigao Plateau, Goa 403206, India

S. C. Mojumdar (✉)
Department of Engineering, University of New Brunswick, Saint John, NB E2L 4L5, Canada
e-mail: scmojumdar@yahoo.com; mojumdar@unbsj.ca

amount of freshly prepared ferrous chloride solution mixed with manganese chloride and zinc chloride solutions was added dropwise with constant stirring in an inert atmosphere. The yellow coloured precipitate thus obtained, was filtered off, washed with ethanol and dried with diethyl ether on suction and then stored in vacuum desiccators.

Characterization

The hydrazine content in the precursor was determined by volumetric analysis using standard 0.025 M KIO_3 solution under Andrew's conditions [45]. The metal contents were determined by chemical analysis. Infrared analysis of the precursor and the ferrite was recorded on a Shimadzu FTIR Prestige 21 series spectrophotometer. Simultaneous TG-DSC analysis of the precursor was recorded on a NETZSCH DSC-TG STA 409 PC thermal analyzer at a heating rate of 10 °C per minute in air. The isothermal mass loss and total mass loss studies along with hydrazine estimation of the precursor were carried out at various predetermined temperatures. The structure and phase purity of the manganese zinc ferrite was determined by Rigaku Ultima IV X-ray diffractometer with CuKα radiations and Ni filter. The saturation magnetization of the "as prepared" ferrite was measured on alternating current hysteresis loop tracer described by Likhite et al. [46] and supplied by M/s Arun Electronics, Mumbai, India.

Results and discussion

Chemical formula fixation of manganese zinc ferrous fumarato–hydrazinate

The analytical data (Table 1) of the precursor, iron = 15.84%, manganese = 4.66%, zinc = 3.69%, hydrazine = 27.47% and total percent mass loss = 67.11% obtained by chemical analysis matches with the calculated values which corresponds to the chemical formula $Mn_{0.6}Zn_{0.4}Fe_2(C_4H_2O_4)_3{\cdot}6N_2H_4$ for manganese zinc ferrous fumarato–hydrazinate complex. The bands in the region 3,304–3,165 cm^{-1} in the infrared spectra of the complex (Fig. 1) are assigned to the N–H stretching frequencies and a band in the range of 1,585–1,560 cm^{-1} is due to NH_2 deformation. The band at 977.9 cm^{-1} is attributed to N–N

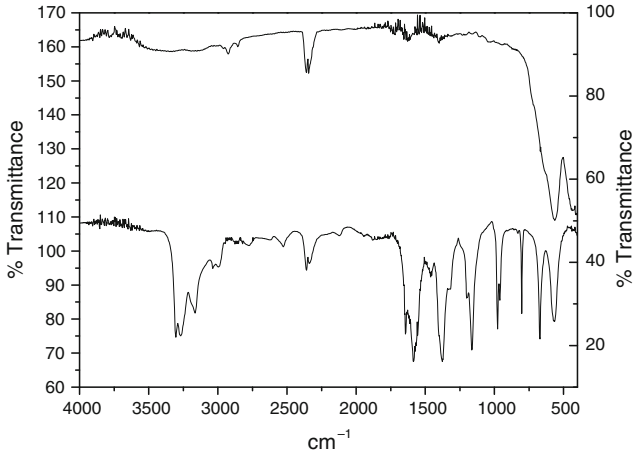

Fig. 1 IR spectra of $Mn_{0.6}Zn_{0.4}Fe_2(C_4H_2O_4)_3{\cdot}6N_2H_4$ complex (*bottom*) and "as prepared" $Mn_{0.6}Zn_{0.4}Fe_2O_4$ (*top*)

stretching of bidentate bridged hydrazine ligand [47, 48]. The wide separation (Δv = 275 cm^{-1}) between $v_{asym}COO^-$ (at 1,643 cm^{-1}) and $v_{sym}COO^-$ (at 1,369 cm^{-1}) of the fumarate groups in the spectrum of the complex supports their monodentate nature [49, 50]. This confirms that the fumarate dianions in the complex coordinate to the metal as bidentate ligand via both the carboxylate groups. Thus, the infrared spectroscopic data enable us to predict that hydrazine acts as a bidentate bridging neutral ligand and fumarate dianion act as a unidentate ligand and hence the complex will invariably be polymeric with the metal ions in the octahedral environment.

Thermal and autocatalytic decomposition of the complex

Manganese zinc ferrous fumarato–hydrazinate precursor decomposes in air, thermally and autocatalytically to form nanosize $Mn_{0.6}Zn_{0.4}Fe_2O_4$.

In autocatalytic decomposition, the precursor is exposed to heat suddenly which results in its decomposition to oxide. The heat is supplied to the precursor by igniting it with a burning splinter wherein precursor catches fire and decomposes autocatalytically to form $Mn_{0.6}Zn_{0.4}Fe_2O_4$ at lower temperature. For this autocatalytic decomposition, the precursor was first spread over a ceramic tile and a burning splinter was brought near to it, when small portion of it caught fire. A red glow that subsequently formed spreads

Table 1 Chemical and total mass loss studies of manganese zinc ferrous fumarato–hydrazinate complex, $Mn_{0.6}Zn_{0.4}Fe_2(C_4H_2O_4)_3{\cdot}6N_2H_4$

Precursor complex	Manganese/%		Zinc/%		Iron/%		Hydrazine/%		Total mass loss/%	
	Obs.	Calc.	Obs.	Calc.	Obs.	Calc.	Obs.	Calc.	Obs.	Calc.
Manganese zinc ferrous fumarato–hydrazinate $Mn_{0.6}Zn_{0.4}Fe_2(C_4H_2O_4)_3{\cdot}6N_2H_4$	4.66	4.67	3.69	3.71	15.84	15.84	27.47	27.26	67.11	66.71

Table 2 TG-DSC, isothermal mass loss studies, and hydrazine analysis data of manganese zinc ferrous fumarato–hydrazinate $Mn_{0.6}Zn_{0.4}Fe_2(C_4H_2O_4)_3{\cdot}6N_2H_4$

Precursor complex	TG		DSC	Remarks	Isothermal mass loss studies		
	Temp. range/°C	Mass loss/%	Peak temperature/°C		Temp. range/°C	Mass loss/%	N_2H_4/%
Manganese zinc ferrous fumarato–hydrazinate $Mn_{0.6}Zn_{0.4}Fe_2(C_4H_2O_4)_3{\cdot}6N_2H_4$	RT–70	1.0	60	Loss of adsorbed moisture	RT–50	0.23	27.46
	70–112	25.5	96.6	Loss of five and half hydrazine molecules	50–70	1.24	27.48
	112–230	10.73	179.4	Loss of half hydrazine and beginning of decarboxylation	70–100	58.76	Complex catches fire
	230–310	24.09	299.2	Decarboxylation	–	–	–
	310–800	6.35	340	Completion of decarboxylation followed by loss of unburned carbon	–	–	–

over the entire bulk completing the total decomposition of the precursor in an ordinary atmosphere to form nanosize manganese zinc ferrite, $Mn_{0.6}Zn_{0.4}Fe_2O_4$ powder. It has been observed in the isothermal mass loss studies (Table 2) that the precursor catches fire at around 100 °C to give a mass loss of above 60% which is due to formation of oxide.

TG, DSC, isothermal mass loss, and hydrazine analysis

The TG and DSC curves (Fig. 2) of the complex in air from room temperature (RT) to 800 °C show four mass loss regions, with two major ones. Initial mass loss of 1.0% till 70 °C is due to the adsorbed moisture, which is also reflected in the DSC which shows very small endotherm in this region. The major mass loss of 25.5% from 70 to 112 °C (Table 2) agrees with the theoretically expected loss of 24.97% due to the elimination of five and half hydrazine molecules. This exothermic loss of hydrazine is indicated in DSC by a sharp exotherm with a peak at 96.6 °C. The mass loss of 10.73% from 112 to 230 °C is due to the loss of remaining half hydrazine molecule simultaneously followed by beginning of decomposition of the dehydrazinated fumarate complex, indicated by exotherm with a peak at 179.4 °C in DSC. The major mass loss of 24.09% in TG curve from 230 to 310 °C can be attributed to oxidative decarboxylation of dehydrazinated fumarate precursor. DSC shows a corresponding sharp exotherm with a peak at 299.2 °C in this region. The mass loss of 6.35% in the region from 310 to 800 °C is due to decomposition of the final traces of precursor or any intermediate formed during decarboxylation along with burning of residual carbon formed during decarboxylation, which is indicated in the DSC by an exothermic hump with peak at 340 °C in this region. Formation of this residual carbon was also confirmed from TG-DSC of "as prepared"

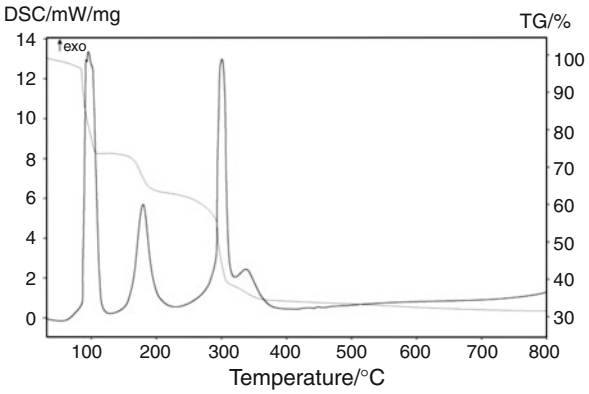

Fig. 2 TG/DSC curves of $Mn_{0.6}Zn_{0.4}Fe_2(C_4H_2O_4)_3{\cdot}6N_2H_4$ complex

$Mn_{0.6}Zn_{0.4}Fe_2O_4$ wherein marginal mass loss on TG curve was observed at 310 to 560 °C with a broad exotherm in this region. The total mass loss (66.67%) obtained from TG curve and by pyrolysis of the complex in air (67.11%) are in well agreement with calculated mass loss (66.71%), considering $Mn_{0.6}Zn_{0.4}Fe_2(C_4H_2O_4)_3{\cdot}6N_2H_4$ as the molecular formula of the complex.

Phase identification, infrared, and magnetic properties of the "as prepared" oxide

The "d" values obtained from the X-ray diffraction pattern of the autocatalytically decomposed end product of the complex (Fig. 3) match well with the reported values for $Mn_{0.6}Zn_{0.4}Fe_2O_4$. The average particle size of "as prepared" $Mn_{0.6}Zn_{0.4}Fe_2O_4$ calculated from XRD using Scherrer formula was found to be 17 nm. The bands in the IR spectra of the "as prepared" $Mn_{0.6}Zn_{0.4}Fe_2O_4$ (Fig. 1) are in agreement with the reported ones [51]. The

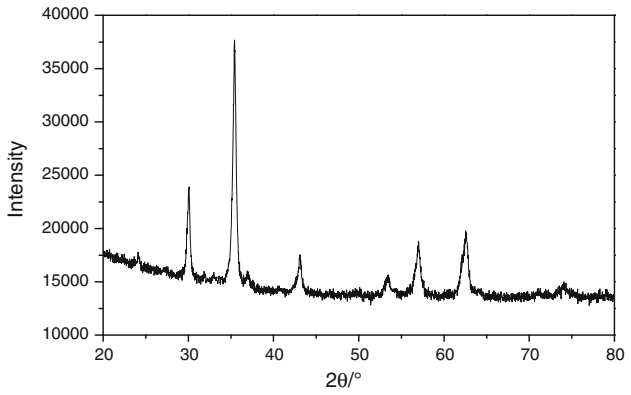

Fig. 3 XRD pattern of "as prepared" $Mn_{0.6}Zn_{0.4}Fe_2O_4$

saturation magnetization of "as prepared" $Mn_{0.6}Zn_{0.4}Fe_2O_4$ was found to be 31.46 emu gm^{-1} which is lower than the reported for bulk one [51]. This lower value of saturation magnetization for $Mn_{0.6}Zn_{0.4}Fe_2O_4$ has been attributed to its nanoparticle size [52].

Conclusions

(1) Nickel manganese zinc ferrous fumarato–hydrazinate can be synthesized easily from sodium fumarate, manganese chloride, zinc chloride, ferrous chloride, and hydrazine hydrate in an inert atmosphere of nitrogen gas at room temperature.
(2) Chemical analysis, total mass loss, and infrared studies of the complex confirms the formation of the complex with formula $Mn_{0.6}Zn_{0.4}Fe_2(C_4H_2O_4)_3{\cdot}6N_2H_4$.
(3) The precursor decomposes autocatalytically once ignited to form nanosize $Mn_{0.6}Zn_{0.4}Fe_2O_4$.
(4) TG-DSC studies of the complex show two-step dehydrazination followed by two-step oxidative decarboxylation to form $Mn_{0.6}Zn_{0.4}Fe_2O_4$.
(5) XRD pattern and IR spectra confirms the formation of the single phase "as prepared" $Mn_{0.6}$ $Zn_{0.4}Fe_2O_4$ nanoparticles.
(6) The broadening of XRD peaks and lower value of saturation magnetization suggest the nanosize nature of "as prepared" $Mn_{0.6}Zn_{0.4}Fe_2O_4$.
(7) The particle size of "as prepared" $Mn_{0.6}Zn_{0.4}Fe_2O_4$ was found to be 17 nm.

References

1. Dalvi BD, Chavan AM. J Therm Anal. 1978;14:331.
2. Langbein H, Eichhorn P. J Therm Anal. 1991;37:993.
3. Poroilo NP, Alley ZG, D'zhardimaliem GL, IvleJa LN, Uflyand LE, Pomogailo AD, et al. Russ Chem Bull. 1997;46(2):362.
4. Dahale ND, Chawla KL, Jayadevan NC, Venugopal V. Thermochim Acta. 1997;293:163.
5. Bhosale DN, Patil VY, Rane KS, Mahajan RR, Bakare PP, Sawant SR. Thermochim Acta. 1998;316:159.
6. Rosenberg AS, Aleksandrova EL, Ivleva NP, Dzhardimalieva GL, Raevskff AV, Kolesova OL, et al. Russ Chem Bull. 1998;47(2):259.
7. Petrochenkova NV, Bukvetskii BV, Mirochnik AG, Karasev VE. Russ J Co-ord Chem. 2002;28(1):64.
8. Deb N. J Therm Anal Calorim. 2005;81:61.
9. Li X, Zou Y-Q. J Chem Cryst. 2005;35(5):351.
10. Badea M, Olar R, Marinescu D, Vasile G. J Therm Anal Calorim. 2005;80:683.
11. Ghodake SR, Ghodake UA, Sawant SR, Suryavanshi SS, Bakare PP. J Magn Magn Mater. 2006;305:110.
12. Randhawa BS, Gandotra K. J Therm Anal Calorim. 2006;85:417.
13. Randhawa BS, Kaur M. J Therm Anal Calorim. 2007;89:251.
14. Jiji ER, Aravindakshan KK. J Therm Anal. 1995;44:65.
15. Kishore K. Indian J Chem. 1969;7:153.
16. Verenkar VMS, Rane KS, Sawant PY. J Mater Sci Mater Electr. 1999;10:133.
17. Rane KS, Verenkar VMS, Pednekar RM, Sawant PY. J Mater Sci Mater Electr. 1999;10:121.
18. Borkar V, Rane KS, Kamat Dalal VN. J Mater Sci Mater Electr. 1993;4:241.
19. Gajapathy D, Patil KC. Mater Chem Phys. 1983;9:423.
20. More A, Verenkar VMS. In: Bahadur D, Vitta S, Prakash O, editors. Inorganic materials: recent advances. New Delhi: Narosa Publishing House; 2006. p. 230.
21. Sawant SY, Kannan KR, Verenkar VMS. In: Pillai CGS, Ramakumar KL, Ravindran PV, Venugopal V, editors. Proceedings of the 13th national symposium on thermal analysis, B.A.R.C., Mumbai. Mumbai: Indian Thermal Analysis Society; 2002. p. 154.
22. Porob RA, Sawant SY, Kannan KR, Verenkar VMS. In: Singh KD, Bharadwaj MS, Ravindran PV, Sali SK, Venugopal V, editors. Proceedings of the 14th national symposium on thermal analysis, Baroda. Mumbai: Indian Thermal Analysis Society; 2004. p. 335.
23. Porob R, Khan SZ, Mojumdar SC, Verenkar VMS. 15th Canadian thermal analysis society's annual workshop and exhibition. Boucherville, Quebec, Canada: National Research Council Canada; 2005.
24. Sawant SY, Mojumdar SC, Verenkar VMS. 16th Canadian thermal analysis society's annual workshop and exhibition, Canada; 2006.
25. Sail GM, Verenkar VMS. 3rd national symposium in chemistry. Chandigarh, India: Punjab University; 2001. p. 133.
26. Ravindranathan P, Patil KC. Thermochim Acta. 1983;71:53.
27. Jiji ER, Aravindakshan KK. Indian J Chem Soc. 1993;70:67.
28. Mahesh GV, Patil KC. Thermochim Acta. 1986;99:188.
29. Patil KC, Gajapathy D, Pai Verneker VR. Mater Res Bull. 1982;17:29.
30. Sharov VA, Nikonenko EA. Russ J Inorg Chem. 1980;25(2):310.
31. Sivasankar BN, Govindarajan S. Synth React Inorg Met-Org Chem. 1994;24:1573.
32. Sivasankar BN. J Therm Anal Calorim. 2006;86(2):385.
33. Verenkar VMS, Rane KS. In: Dharwadkar SR, Bharadwaj SR, Mukherjee SK, Sood DD, editors. Proceedings of the 10th national symposium on thermal analysis, DMSRDE; Kanpur. Mumbai: Indian Thermal Analysis Society; 1995. p. 171.
34. Verenkar VMS, Rane KS. In: Dharwadkar SR, Bharadwaj SR, Mukherjee SK, Sood DD, editors. Proceedings of the 10th national symposium on thermal analysis, DMSRDE; Kanpur, 1995. Mumbai: Indian Thermal Analysis Society; 1995. p. 175.
35. Rane KS, Verenkar VMS. Bull Mater Sci. 2001;24:39.

36. Verenkar VMS, Rane KS. In: Ravindran PV, Sundersanan M, Misra NL, Venugopal V, editors. Proceedings of the 12th national symposium on thermal analysis, Gorakhpur. Mumbai: Indian Thermal Analysis Society; 2000. p. 194.
37. Sawant SY, Verenkar VMS, Mojumdar SC. J Therm Anal Calorim. 2007;90:669.
38. Gawas U, Bhattacharya S, More A, Verenkar VMS. In: Lokhande Dr CD, editor. Proceedings of the international conference on advanced materials and applications. Kolhapur, India; 2007. p. 86.
39. Porob RA, Khan SZ, Mojumdar SC, Verenkar VMS. J Therm Anal Calorim. 2006;86:605.
40. More A, Verenkar VMS, Mojumdar SC. 18th Canadian thermal analysis society's annual workshop and exhibition, Canada; 2008. p. 28.
41. Gawas UB, Verenker VMS, Mojumdar SC. 18th Canadian thermal analysis society's annual workshop and exhibition, Canada; 2008. p. 47.
42. More A, Verenkar VMS, Mojumdar SC. J Therm Anal Calorim. 2008;94:63.
43. Gawas UB, Mojumdar SC, Verenker VMS. J Therm Anal Calorim. 2009;96(1):49.
44. Gonsalves LR, Verenker VMS, Mojumdar SC. J Therm Anal Calorim. 2009;96(1):53.
45. Vogel's, Text book of quantitative inorganic analysis (Revised by Jeffery GH, Bassettv, Mendham J and Denney RC), 5th edn. Longman, UK; 1989. p. 402.
46. Likhite SD, Radhakrishnamurthy C, Sahasrabudhe PW. Rev Sci Instr. 1965;25:302.
47. Braibanti A, Dallavalle F, Pellinghelli MA, Leporati E. Inorg Chem. 1968;7:1430.
48. Tsuchiya R, Yonemura M, Uehera A, Kyuno E. Bull Chem Soc Jpn. 1974;47(3):660.
49. Sivasankar BN, Govindarajan S. Z Naturforsch B. 1994;49(7):950.
50. Nakamoto K. Infrared and Raman spectra of inorganic and coordination compounds. New York: Wiley; 1978.
51. Tangsali RB, Keluskar SH, Naik GK, Budkuley JS. Int J Nanosci. 2004;3(4–5):589.
52. Srivastava P, Kumar J. In: Bahadur D, Vitta S, Prakash O, editors. Inorganic materials: recent advances. New Delhi: Narosa Publishing House; 2006; p. 423.